Eur. Phys. J. AP **5**, 163–169 (1999)

THE EUROPEAN PHYSICAL JOURNAL APPLIED PHYSICS

Time-resolved studies of short pulse laser-produced plasmas in silicon dioxide near breakdown threshold

C. Quoix[1], G. Grillon[1], A. Antonetti[1], J.-P. Geindre[2], P. Audebert[2], and J.-C. Gauthier[2,a]

[1] Laboratoire d'Optique Appliquée (LOA)[b], École Polytechnique, ENSTA, rue de la Hunière, 91167 Palaiseau, France

[2] Laboratoire pour l'Utilisation des Lasers Intenses (LULI)[c], École Polytechnique, CEA, Université Paris VI, 91128 Palaiseau, France

Received: 2 October 1998 / Revised and Accepted: 29 October 1998

Abstract. Using the technique of frequency-domain interferometry, we demonstrate a new way of studying laser-induced breakdown at the surface of dielectric materials. A theoretical model based on electron production by multiphoton ionisation, inverse bremsstrahlung heating, and collisional ionisation is in quantitative agreement with both the detailed time variation of the dielectric constant and the pulse width variation of the fluence threshold. From the complex reflection coefficient measured with the two probe pulse polarisations in quadrature, we deduce the time variation of the dielectric constant of silica during breakdown.

PACS. 52.50.Jm Plasma production and heating by laser beams – 78.47.+p Time-resolved optical spectroscopies and other ultrafast optical measurements in condensed matter – 77.22.Jp Dielectric breakdown and space-charge effects

1 Introduction

The non-linear optical properties of dielectric materials, particularly glass and fused silica, are of considerable interest because of their role in high-power laser applications where damage to optical components, due to laser-induced breakdown, limits the whole laser system performance. In the nanosecond and sub-nanosecond laser pulse regime, a $\tau^{1/2}$ dependence of the threshold damage fluence upon pulse duration has been experimentally demonstrated (for a review see [1] and references therein). This particular scaling law is obtained because the controlling rate for conduction band electron energy losses is that of electron thermal conduction for laser pulse durations very much longer than the electron-phonon energy transfer time to the lattice. Recently, the numerous applications of chirped-pulse amplification (CPA) to ultrahigh intensity laser interaction physics [2,3] have brought laser-induced breakdown experiments to the picosecond and sub-picosecond time scale [1,4,5], down to 5 fs laser pulse durations [6]. In this new regime, heat diffusion plays a negligible role during the interaction so that energy transfer (heat and impulse) to the target material and the heat-affected zone (HAZ) dimensions are minimised [7,8]. Applications for nanometer-precision material processing, particularly through laser ablation, look very promising [9].

Previous measurement methods for laser-induced breakdown threshold studies relied on light microscopy [1], a combination of light and electron scanning microscopy [6], the change of transmission through the sample [4] or reflective optical probing of the damage with an auxiliary laser pulse [5,10]. The most objective methods used so far to evaluate the threshold fluence for plasma formation are based on the fact that the ablated material volume, or the area of the damaged spot, scale linearly with the laser fluence. Extrapolating the linear regression to zero gives the threshold with a rather high degree of confidence [6]. However, with these methods, no information can be obtained on the temporal dynamics of the breakdown process, only the value of the threshold can be determined.

The great value of femtosecond pump probe techniques in giving access to time-resolved studies of ultrashort pulse laser perturbation of optical properties of semiconductors [10,11], metals [12,13], and dielectrics [14–16] is now well-recognised. For transparent materials, when the threshold fluence for breakdown is exceeded, a dense plasma is formed, which causes a marked jump in the optical reflectivity. This has been interpreted [17], within the Drude model approximation, through variations of the material dielectric constant with the electron density and the electron collisional rate. To our knowledge, the first attempt to apply pump-probe reflectivity measurements to

[a] e-mail: gauthier@greco2.polytechnique.fr

[b] UMR 7639 CNRS

[c] UMR 7605 CNRS

the laser-induced dielectric breakdown problem was made by von der Linde and Schüler [5]. It was found that the reflectivity measured 200 fs after the peak of the laser pump was roughly constant above a certain intensity threshold ($\approx$ 100 TW/cm^2). However, the information on breakdown dynamics contained in the transient reflectivity was not fully exploited.

Our work significantly extends these earlier studies by introducing the simultaneous measurement of the reflectivity and of the phase shift of an ultrashort duration probe pulse during breakdown. Optical methods giving access to the phase shift of a probe beam in transmission or reflection have shown their usefulness in solid state physics [16,18,19] and plasma physics [20–22]. Here, the phase shift of the probe beam gives a direct measurement of the time variation of the electron density during laser-induced ionisation [20]. We use the technique of frequency-domain interferometry giving the phase shift between a pair of reflected probe pulses from the plasma produced on fused silica by variable pulse duration laser interaction. Our aim is not to provide a systematic study of the variation of the breakdown laser fluence threshold with pulse duration, wavelength, or the nature of the material. The important point in this work is the study of the potentiality of femtosecond frequency-domain interferometry to get new informations on breakdown dynamics and plasma formation on the surface of dielectric materials.

2 Experimental system

The experiments were carried out with the LOA Ti:Al_2O_3 CPA laser in Palaiseau [23]. This laser delivers nominally 120 fs duration, 60 mJ energy, 800 nm wavelength, 10 Hz repetition rate pulses. The laser intensity contrast ratio was measured to be better than 10^{-8} (at 2 ps before the main pulse) by high-dynamics third order autocorrelation techniques. This system was also used to measure the pulse duration. The main laser pulse, p-polarised, was focused onto the target at 7° incidence angle by a 40 cm ($f/10$) focal length MgF_2 lens. The pump laser pulse irradiance was varied from 5×10^{12} to 5×10^{14} W/cm^2 by inserting variable diameter circular diaphragms in the beam path. The full width at half maximum (FWHM) size of the spot was measured by equivalent focal plane microscopy from the first dark Airy disk diameter. It was found very close to the diffraction limit fixed by the size of the diaphragm delimiting the beam. Two different grating compressors were used, one to provide the probe laser beam of fixed temporal duration ($\approx$ 150 fs) and the other to provide the pump laser beam, the duration of which could be changed by finely tuning the dispersive path length (0.12–2.5 ps). We used fused silica (SiO_2) microscope slides as a target material. No particular attention was paid to the purity of the target samples because we were not primarily interested in reproducing the previously measured breakdown thresholds. It turned out afterwards that our estimates of laser fluence thresholds were in good agreement with the results of Stuart *et al.* [1], showing that the contribution of the intrinsic properties of fused silica were dominant.

To measure the rapid change of the optical properties of fused silica during breakdown with high spatial and temporal resolution, we have used the technique of frequency-domain interferometry [20,24], extended to allow simultaneous measurements of the phase shift for the two (s and p) probe polarisations [18,25]. This technique has also been used recently [16,26], at laser pump irradiances of a few TW/cm^2, to study the laser-induced carrier trapping dynamics in wide band-gap crystals such as fused silica. The frequency-doubled 400 nm wavelength probe pulses were separated in a Michelson interferometer set to give a constant delay of 6.1 ps between the reference (arriving before the pump) and the probe (arriving after the pump) pulses. The breakdown plasma illuminated by the twin probe pulses was imaged on the entrance slit of an imaging spectrograph. The imaging lens provides spatial resolution along a diameter of the pump focal spot, parallel to the plane of incidence. The temporally separated pulses can interfere owing to the dispersion of the spectrograph grating which, acting as a pulse stretcher, broadens the pulses to make them overlap in time. The interference pattern was recorded by a cooled 16 bits CCD camera. A specially designed optical system changed the circular shape of the probe beam into a slit-like shape, elongated along the spatial resolution direction, parallel to the incidence plane [24]. Accordingly, the along-the-slit focal spot size of the probe and reference beams was several times larger than the pump focal spot size to allow uniform illumination of the region under test. By realising a virtual slit in the far field of the target, this particular arrangement greatly reduced the spatial phase non-uniformities of the probe beam and helped to avoid the parasitic effects of the defects (small indentations) of the entrance slit of the spectrograph. The angle of incidence of the twin probe pulses was 46.4° from target normal. The target was moved between each shot to provide a fresh surface to successive laser shots. The resolution of our measurement system was about 2 μm along the focal spot diameter [20]. An interferogram was obtained for each delay between the pump and the twin probes. The phase as a function of radial position was calculated on-line from the digitized image by inverse Fourier transform techniques.

Damage always occurred at the central part of the focal spot corresponding to the peak of the Gaussian intensity profile, indicating that small size surface defects did not contribute to the measured threshold. Figure 1 shows the phase difference between the twin pulses, measured in this central part, obtained for pump pulse durations of 0.16 ps, 0.76 ps, and 2.2 ps. The probe pulses are p-polarised. In this particular measurement, no effort was made to determine the zero point of the time scale. Figures 1b and 1c show clearly the effect of changing the laser irradiance on the phase difference dynamics. Before the breakdown time, the phase difference is zero. Then, during the rising edge of the laser pulse, the electron density increases sharply. This leads to a strong increase of the phase difference. At late times, the phase difference variation is governed by the expansion of the plasma.

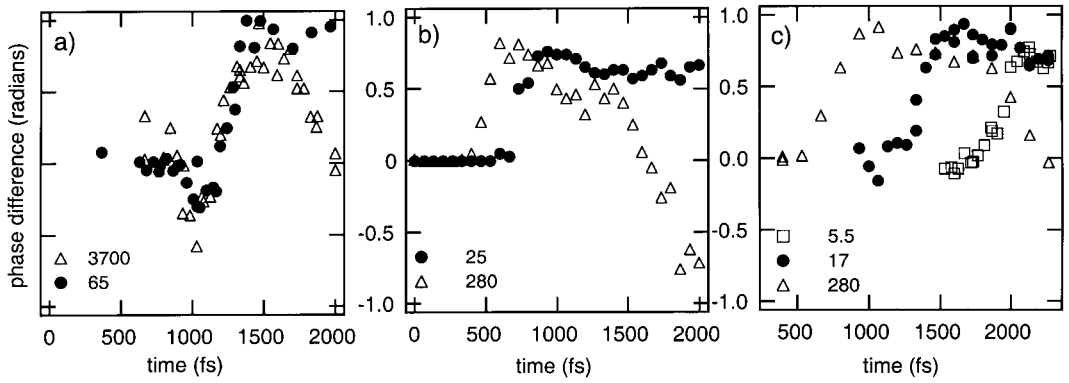

Fig. 1. Time-resolved phase measurements for three pulse durations and various laser irradiances in TW/cm^2. (a) Pump pulse duration of 0.16 ps; (b) 0.76 ps; (c) 2.2 ps.

Table 1. Breakdown fluence of fused silica in J/cm^2 as a function of pulse duration.

pulse duration	this work	von der Linde [5]	Stuart[1]
150 fs	-	3.3	1.8
760 fs	1.7 ± 0.3	-	2.2
2200 fs	2.5 ±0.3	-	3

This can be clearly seen in Figure 1b for the larger irradiance of 2.8×10^{14} W/cm^2. The detailed variation of the phase with plasma parameters and laser characteristics has been described at length in a previous publication [20]. For higher pump intensities in Figures 1b and 1c, the increasing edge of the phase is observed to move to earlier times, as might be expected. In Figure 1a, the probe and pump laser pulse durations being comparable, no significant time shift of the phase jump is found when the laser irradiance is changed from 65 to 3 700 TW/cm^2. The small negative phase shift around 1 ps can be attributed to nonlinear mixing at peak time of the pump and probe pulses. This was observed only for the shorter pulse durations and higher laser intensities, providing an elegant way to assess the temporal coincidence of the pump and probe pulses. The effect of the finite duration of the probe pulse on the measured phase shift transient during breakdown ionisation has been investigated in reference [27]. Accordingly, the time constant of the phase jump seems to be time-resolution limited. The magnitude of the phase change during breakdown is virtually independent of laser irradiance in the range we have studied. This will be investigated in the next section. From the measured laser energy, we determined the threshold laser fluence for breakdown by integrating the measured pulse shape up to the time where 50% of the total phase jump was reached. Results are given in Table 1; they are compared to the previously measured values [1,5].

3 Theoretical model

Optical breakdown in the short pulse regime can be described in terms of:

(i) electron excitation in the conduction band by multiphoton and electron impact processes;
(ii) heating of free electrons in the conduction band by laser radiation;
(iii) transfer of electron energy to the lattice.

A model based on the numerical simulation of the full kinetic equation incorporating the ionisation and heating processes has been recently proposed by Stuart *et al.* [1]. Results show that the ionisation rate is linearly proportional to the laser irradiance. The linear scaling of the avalanche with intensity was confirmed recently in reference [6].

Here, we use a variant of the rate equation formalism [1] which, in our case, follows the time evolution of the electron energy density. We restrict our model to describe single ionisation, the corresponding free electron density being larger than the critical density $n_c = m_e\epsilon_0\omega^2/e^2$ where ω is the laser pulsation. Critical density n_c is a commonly accepted density threshold condition that breakdown occurs [4]. The total electron energy density can be written:

$$\xi = \frac{3}{2} n_e k T_e + n_e U_0 \quad (1)$$

$$d\xi/dt = \frac{\omega}{2}\epsilon_0 \mathrm{Im}(\epsilon)|E|^2 + W(N_0 - n_e)(U_0 + kT_e) \quad (2)$$

where N_0 and U_0 are the atomic number density and the band gap energy of SiO_2, respectively, ϵ is the dielectric constant, E is the electric field amplitude, and W is the laser-induced ionisation rate. The first term on the right hand side of equation (2) corresponds to inverse bremsstrahlung laser absorption: it is proportional to laser irradiance [1]; the second term describes laser ionisation by multi-photon and/or tunnel ionisation directly related to the laser field. Because we restrict the validity of our model to the description of picosecond and sub-picosecond laser interaction not far from breakdown conditions, we neglect the energy losses due to electron energy transfer to the

lattice, the thermal diffusion effects, the electron recombination, and the hydrodynamic expansion of the plasma in equation (2). We can also assume that the temperature of the electrons in the conduction band is limited to the few electronvolts found from the Saha equation and is time-independent [28,29] because the electron energy gained in the laser field is used to ionise the neutral atoms of the material. Combining equations (1, 2), we get:

$$dn_e/dt = \frac{1}{(3/2kT_e + U_0)}\frac{\omega}{2}\epsilon_0 \mathrm{Im}(\epsilon)|E|^2 + \frac{1}{(3/2kT_e + U_0)}W(N_0 - n_e)(U_0 + kT_e). \quad (3)$$

As in reference [12] we use the expression of the dielectric constant given by the Drude model:

$$\epsilon = \epsilon_0 - \frac{n_e/n_c}{1+\nu^2/\omega^2} - \imath\frac{n_e/n_c\nu/\omega}{1+\nu^2/\omega^2} \quad (4)$$

where ϵ_0 is the dielectric constant of unperturbed SiO_2 and ν the electron-phonon scattering collision frequency [30]. Substituting equation (4) into equation (3), one gets a simplified expression similar to the one proposed by Stuart *et al.* [1]:

$$dn_e/dt = \alpha I(t) n_e + P(I)(1 - n_e/N_0), \quad (5)$$

where $P(I)$ is the multi-photon ionisation rate. The relative role of multi-photon ionisation and electron impact in ultrashort pulse breakdown has been discussed in reference [4]. For 800 nm light, six-photon absorption cross-section values were not available until recently [6]. Mike Perry *et al.* [31] have shown that ionisation of the first ion stage of noble gases is well-described by Keldysh-like theories. The photo-ionisation process is sensitive to the adiabaticity (Keldysh) parameter $\gamma = \omega\sqrt{2mU_0}/eE$ where E is the peak laser field. For the range of parameters close to breakdown, $\gamma \geq 1$, indicating that multi-photon ionisation dominates over barrier-suppression and tunnel ionisation. Here, we have used an expression of the laser ionisation cross-section [32] which cover the multi-photon and tunnelling regimes of ionisation. For $\gamma \gg 1$, the ionisation cross-section can be well-approximated by the six-photon ionisation rate $P_6(I) = 6 \times 10^{16}$ cm^{-3}ps^{-1} (cm^2/TW)^6. This value is comparable to the one quoted in [1] for slightly different laser wavelengths but about 8 orders of magnitude larger than the value reported by Lenzner *et al.* [6]. We note that this low value of the laser ionisation cross-section was put forward in order to explain "anomalously high" sub-10 fs laser pulse breakdown thresholds. This is an interaction regime very different from ours.

Equation (5) was numerically solved as a function of space and time for various values of pump laser intensities and pulse shapes. The first 500 nm of the silica target exposed to the pump and probe lasers were treated as a multi-layer material, the dielectric constant of each layer being calculated according to equation (4). The bulk of the target was simulated by an unperturbed silica substrate.

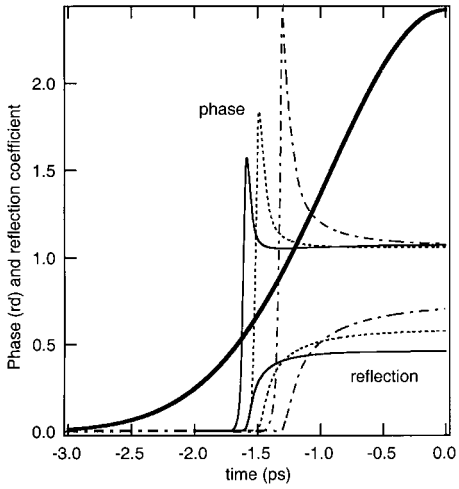

Fig. 2. Time evolution of the phase and the amplitude of the reflected probe pulse for 2.2 ps duration laser pulse as a function of the electron-phonon momentum transfer collision rate. Dashed-dotted line: $\nu = 10^{15}$ s^{-1}, dotted line: $\nu = 2 \times 10^{15}$ s^{-1}, solid line: $\nu = 3 \times 10^{15}$ s^{-1}. The laser irradiances is 20 TW/cm^2. *p*-polarised probe light at 400 nm.

The electron-phonon scattering frequency was considered as a spatially constant, adjustable parameter. A multilayer dielectric propagation code [33] was used to evaluate the field in each layer. In doing so, we assumed implicitly that the hydrodynamic motion of the vacuum-target interface was negligible during the interaction. Then, equation (5) was solved self-consistently and the new electron density was used to evaluate a new set of multilayer dielectric constants. A probe beam at 400 nm, of negligible intensity, was also propagated onto the target with 45° incidence angle. The amplitude and the phase shift upon reflection of the 45° probe beam were calculated as a function of the delay between the pump pulse and the probe pulse. The consistency of the model was checked against the results of Stuart *et al.* [1] at 1 053 nm and 526 nm.

4 Results and discussions

Figure 2 shows the instantaneous phase shift and reflection coefficient of the probe beam as a function of time for three different values of the electron-phonon scattering frequency. The finite duration of the probe pulse was not taken into account in the calculation. The temporal shape of the pump pulse is also shown. The higher the collision frequency, the sooner (lower threshold fluence) breakdown occurs, as expected. There is no significant variation of the asymptotic phase with collision frequency. This is related to the fact that the phase shift is more sensitive, within the Drude model approximation, to the electron density variation. On the contrary, the reflection coefficient obtained a few hundreds of fs after breakdown varies with the collision frequency, lower absorption (higher reflectivity) being obtained for lower collisionality. There is a distinct delay between the onset of the phase shift jump and the change in reflectivity which corresponds to the time it takes to

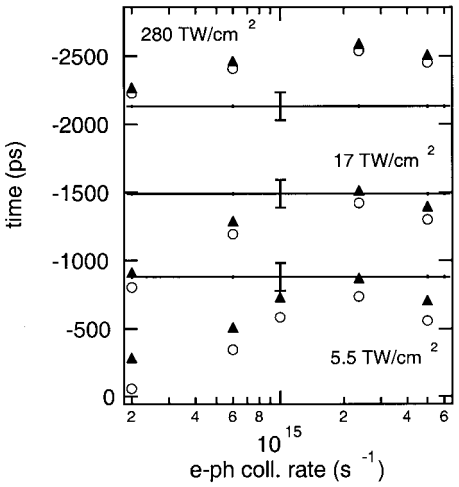

Fig. 3. Calculated breakdown times (with respect to the peak of the 2.2 ps duration laser pulse) as a function of the electron-phonon momentum transfer collision rate. Filled symbols: 3 eV; Open symbols: 1 eV electron temperature. From top to bottom, the laser irradiances are 280, 17, and 5.5 TW/cm^2. Horizontal lines are the experimental results with error bars.

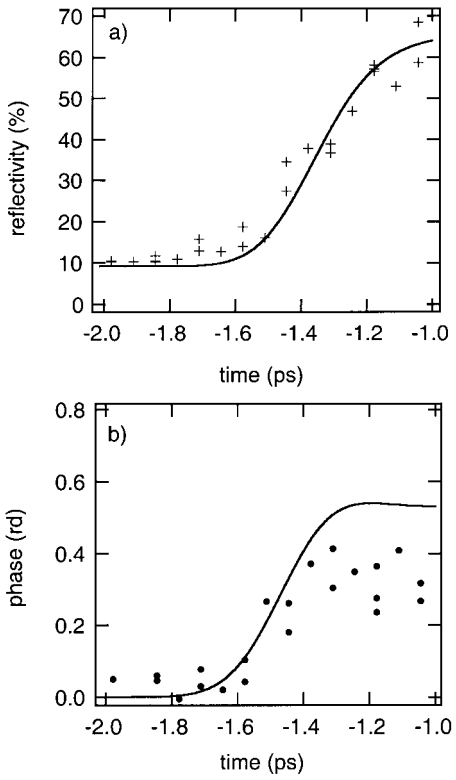

Fig. 4. Time-resolved reflectivity (a) and phase (b) measurements for 2.2 ps pump pulse duration and 1.7×10^{13} W/cm^2 irradiance for *s*-polarised light. The solid line is the result of the model described in the text.

reach electron densities which give a large negative value to the real part of the dielectric constant.

The calculated breakdown time (taken at the 50% level of the asymptotic phase change) is compared to experimental results in Figure 3. In the calculations, we changed the electron-phonon collision rate and the electron temperature. For low irradiances, below ten times the threshold fluence, the measured breakdown time matches the calculations for a collision rate of about 2.5×10^{15} s^{-1}. This value is comparable with calculated estimates [16,30, 26] of the momentum relaxation rate of acoustic phonons in SiO_2 for electron energies of a few electronvolts. At higher irradiance (*cf.* the top curve in Fig. 3), the validity of our model is questionable because the electron temperature is getting larger than the band gap energy, leading to suprathermal electron transport [30], and hydrodynamic effects come into play for the pulse duration we have used. In addition, the higher the laser intensity, the better the shape of the early wing of the laser pulse has to be known in order to obtain an accurate value of the threshold fluence for breakdown. The variation of the breakdown time with the (assumed) electron temperature is small, except at near-threshold irradiance. The breakdown time maximum, followed by a decrease at large collision rates, is easily explained by the fact that the imaginary part of the Drude dielectric function is maximum for $\nu/\omega \sim 1$. We have checked the sensitivity of our results to the laser ionisation rate $P(I)$ by using the optical ionisation cross-section measured in reference [6]. With this remarkably low value of the cross-section, no agreement was found with experiment even for unrealistic values of the electron phonon collision rate.

We have plotted in Figures 4 and 5 the measured and calculated evolution of the phase shift and of the reflectivity for *s*- and *p*-polarised probe light as a function of the time delay between the pump and probe pulses. Here, we took into account the finite duration of the probe pulse in the calculations. The collisional frequency is 2.5×10^{15} s^{-1}, as determined previously. The agreement is satisfactory regarding the relative simplicity of the breakdown model we have employed. In passing, it is noteworthy that experiments clearly show the time delay, exhibited in the modelling, between the onset of the reflectivity and phase changes. Knowing the amplitude and the phase of the reflection coefficient for the two polarisations in quadrature, it is possible [33] to extract the time variation of the dielectric constant of SiO_2 by using the Fresnel formulas for the reflection coefficient. This procedure is only valid for a sharp vacuum-plasma interface. This is done in Figure 6 where we have plotted the real and imaginary part of the dielectric constant for a laser intensity of 65 TW/cm^2 and a pulse duration of 160 fs. This is about 3 times the breakdown threshold and, for this pulse duration, hydrodynamic effects remain small for times $\pm$100 fs around the peak of the pump laser. Before breakdown, the real part of the dielectric constant is close to the square of the refractive index ($\epsilon_0 \sim 2.25$) and the imaginary part is zero, as expected. Then, around 1 ps there is a small drop of the imaginary part of the dielectric constant related to the nonlinear mixing of the pump and the probe pulse described previously. This is followed by a sharp rise at breakdown time corresponding to the electron density

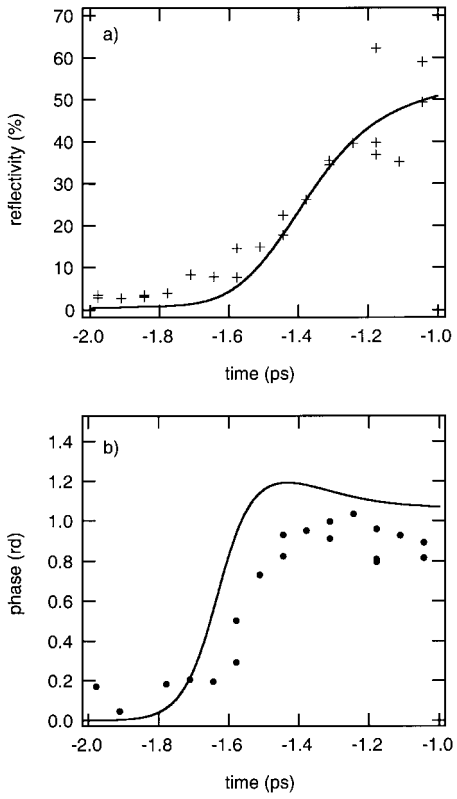

Fig. 5. Time-resolved reflectivity (a) and phase (b) measurements for 2.2 ps pump pulse duration and 1.7×10^{13} W/cm^2 irradiance for p-polarised light. The solid line is the result of the model described in the text.

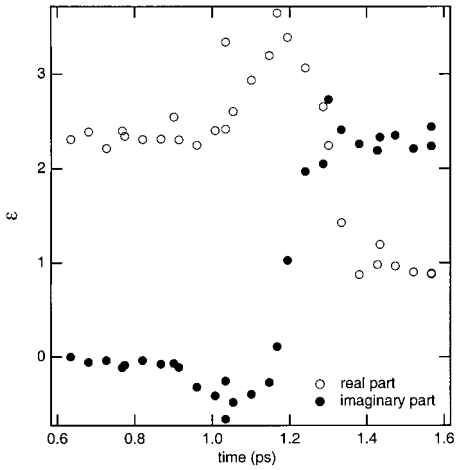

Fig. 6. Time-resolved real and imaginary part of the dielectric constant of silica during breakdown for 0.16 ps pump pulse duration and 6.5×10^{13} W/cm^2 irradiance.

increase. At the same time, the real part of the dielectric constant drops. Asymptotically, it does not reach negative values as expected because the vacuum-silica interface motion and finite thickness adds Doppler and plasma contributions to the phase shift [20]. There is a distinct peak in the real part of the dielectric function before it drops. We do not have an explanation for this effect to date but one cannot exclude some perturbation of the measurement by the nonlinear mixing of the pump and the probe pulse at peak time coincidence.

5 Concluding remarks

From the above results, the following remarks and perspectives can be drawn:

- dual quadrature frequency-domain interferometry is a very powerful technique to study optical breakdown threshold with high spatial and temporal resolution. By measuring simultaneously the reflectivity and the phase of a time-delayed probe pulse in the two polarisations, we have have shown the possibility of a direct determination of the time variation of the complex dielectric function of silica during breakdown;
- the rate equation formalism, in which the time variation of the total electron (valence and conduction) energy density is followed, gives a powerful description of laser-induced breakdown. Multi-photon ionisation provides the seed electrons in the conduction band and inverse bremsstrahlung heating controlled by electron-acoustic phonon scattering develops the electron avalanche. Comparing the results of the model with experiment, we have access to the electron scattering rate. Here we have assumed a constant electron temperature during breakdown but the extension of the procedure analysis to time-varying temperature has been successfully demonstrated recently [34];
- in the present work, the time duration of the probe laser beam was too long to fully exploit the technique in studying sub-100 fs laser-induced breakdown. With the newly developed high-intensity short pulse laser [35] at LOA, this type of study would be possible in the near future.

It is a pleasure to acknowledge fruitful discussions with Ph. Balcou on multi-photon ionisation and Alessandro Mirone for his help in the use of the multilayer model. We are indebted to the laser staff of Laboratoire d'Optique Appliquée for their continuous support. This work was financed by the Centre National de la Recherche Scientifique and by the European Community under the Training and Mobility in Research programme ERBFMRX CT96-0080.

References

1. B.C. Stuart, M.D. Feit, S. Herman, A.M. Rubenchik, B.W. Shore, M.D. Perry, Phys. Rev. B **53**, 1749 (1996); B.C. Stuart, M.D. Feit, S. Herman, A.M. Rubenchik, B.W. Shore, M.D. Perry, J. Opt. Soc. Am. B **13**, 459 (1996).
2. G. Mourou, D. Umstadter, Phys. Fluids B **4**, 2315 (1992).
3. M.D. Perry, G. Mourou, Science **264**, 917 (1994).
4. D. Du, X. Liu, G. Korn, J. Squier, G. Mourou, Appl. Phys. Lett. **64**, 3071 (1994).

5. D. von der Linde, H. Schüler, J. Opt. Soc. Am. B **13**, 216 (1996).
6. M. Lenzner, J. Krüger, S. Sartania, Z. Cheng, Ch. Spielmann, G. Mourou, W. Kautek, F. Krausz, Phys. Rev. Lett. **80**, 4076 (1998).
7. W. Kautek, J. Krüger, Proc. SPIE **2207** (SPIE Press, Bellingham, Washington, 1994), p. 60.
8. B.N. Chichkov, C. Momma, S. Nolte, F. von Alvensleben, A. Tünnermann, Appl. Phys. A **63**, 109 (1996).
9. C. Momma, B.N. Chichkov, S. Nolte, F. von Alvensleben, A. Tünnermann, H. Welling, B. Wellegehausen, Opt. Commun. **129**, 134 (1996).
10. M.C. Downer, R.L. Fork, C.V. Shank, J. Opt. Soc. Am. B **2**, 595 (1985).
11. D. Hulin, M. Combescot, J. Bok, A. Migus, J.Y. Vinet, A. Antonetti, Phys. Rev. Lett. **52**, 1998 (1984).
12. X.Y. Wang, M.C. Downer, Optics Lett. **20**, 1450 (1992).
13. O.L. Landen, W.E. Alley, Phys. Rev. A **48**, 5089 (1992).
14. B.-T.V. Vu, A. Szoke, O.L. Landen, Optics Lett. **18**, 723 (1993).
15. B.-T.V. Vu, O.L. Landen, A. Szoke, Phys. Plasmas **2**, 476 (1995).
16. P. Martin, S. Guizard, Ph. Daguzan, G. Petite, P. D'Oliveira, P. Meynadier, M. Perdrix, Phys. Rev. B **55**, 5799 (1997) and references therein.
17. R. Fedosejevs, R. Ottmann, R. Sigel, G. Kühnle, S. Szatmari, F.P. Schäfer, Appl. Phys. B **50**, 79 (1990).
18. L. Lepetit, G. Chériaux, M. Joffre, J. Opt. Soc. Am. B **12**, 2467 (1995).
19. P. Audebert, P. Daguzan, A. Dos Santos, J.-C. Gauthier, J.-P. Geindre, S. Guizard, G. Hamoniaux, K. Krastev, P. Martin, G. Petite, A. Antonetti, Phys. Rev. Lett. **73**, 1990 (1994).
20. P. Blanc, P. Audebert, F. Falliès, J.-P. Geindre, J.-C. Gauthier, A. Dos Santos, A. Mysyrowicz, A. Antonetti, J. Opt. Soc. Am. B **13**, 118 (1996).
21. R. Evans, A.D. Badger, F. Falliès, M. Mahdieh, T. Hall, P. Audebert, J.-P. Geindre, J.-C. Gauthier, A. Mysyrowicz, G. Grillon, A. Antonetti, Phys. Rev. Lett. **77**, 3359 (1996).
22. J.R. Marquès, J.-P. Geindre, F. Amiranoff, P. Audebert, J.-C. Gauthier, A. Antonetti, G. Grillon, Phys. Rev. Lett. **76**, 3566 (1996).
23. C. Le Blanc, G. Grillon, J.-P. Chambaret, A. Migus, A. Antonetti, Optics Lett. **18**, 140 (1993).
24. J.-P. Geindre, P. Audebert, A. Rousse, F. Falliès, J.-C. Gauthier, A. Mysyrowicz, A. Dos Santos, G. Hamoniaux, A. Antonetti, Optics Lett. **19**, 1997 (1994).
25. S. Bastiani, A. Rousse, J.-P. Geindre, P. Audebert, C. Quoix, G. Hamoniaux, A. Antonetti, J.-C. Gauthier, Phys. Rev. E **56**, 7179 (1997).
26. P. Daguzan, Ph.D. thesis, University of Paris, 1996.
27. J.-R. Marquès, F. Dorchies, F. Amiranoff, P. Audebert, J.-C. Gauthier, J.-P. Geindre, A. Antonetti, T.M. Antonsen Jr., P. Chessa, P. Mora, Phys. Plasmas **5**, 1162 (1998).
28. M. Newstein, N. Solimene, IEEE J. Quant. Electr. **17**, 2085 (1981).
29. B.-T.V. Vu, O.L. Landen, A. Szoke, Phys. Rev. E **47**, 4 (1995).
30. D. Arnold, E. Cartier, D.J. di Maria, Phys. Rev. B **45**, 1477 (1992).
31. M.D. Perry, O.L. Landen, A. Szöke, E.M. Campbell, Phys. Rev. A **37**, 747 (1988).
32. F.A. Ilkov, J.E. Decker, S.L. Chin, J. Phys. B: At. Mol. Opt. Phys. **25**, 4005 (1992).
33. M. Born, E. Wolf, *Principles of Optics* (Pergamon Press, Oxford, 1993).
34. C. Quoix, Ph.D. thesis, University of Paris, 1998 (available upon request to the corresponding author).
35. J.-P. Chambaret *et al.*, Optics Lett. **21**, 1921 (1996).